

Density functional theory of charged, hard-sphere fluidsDirk Gillespie,^{1,2,*} Wolfgang Nonner,^{2,†} and Robert S. Eisenberg^{1,‡}¹*Department of Molecular Biophysics and Physiology, Rush University, 1750 West Harrison Street, Suite 1291, Chicago, Illinois 60612, USA*²*Department of Physiology and Biophysics, University of Miami School of Medicine, P.O. Box 016430, Miami, Florida 33101-6430, USA*

(Received 18 April 2003; published 19 September 2003)

An approximate electrostatic (ES) excess free energy functional for charged, hard sphere fluids is presented. This functional is designed for systems with large density variations, but may also be applied to systems without such variations. Based on the Rosenfeld method of perturbation about a bulk (homogeneous) reference fluid [Y. Rosenfeld, *J. Chem. Phys.* **98**, 8126 (1993)], the new ES functional replaces the reference fluid densities with a functional of the particle densities, called the RFD functional. The first-order direct correlation function (DCF) in the particle densities is computed using as input the first- and second-order DCFs in $\{\bar{\rho}_i(\mathbf{x})\}$, the inhomogeneous densities defined by the RFD functional. Because this formulation imposes no *a priori* constraints on the form of the RFD functional—it is valid for any choice of $\{\bar{\rho}_i(\mathbf{x})\}$ —the RFD functional may be chosen (1) so that the input DCFs (that is, DCFs in $\{\bar{\rho}_i(\mathbf{x})\}$) may be approximated and (2) so the combination of $\{\bar{\rho}_i(\mathbf{x})\}$ and input DCFs yields a good estimate of the first-order DCF in the particle densities. In this way, the general problem of finding the excess free energy functional has been replaced by the specific problem of choosing a RFD functional. We present a particular RFD functional that, together with bulk formulations for the input DCFs, accurately reproduces the results of Monte Carlo simulations.

DOI: 10.1103/PhysRevE.68.031503

PACS number(s): 61.20.Gy, 61.20.Qg

I. INTRODUCTION

Fluids of charged, hard spheres are widely used to represent physical systems such as electrolyte solutions. In bulk (homogeneous) systems, these fluids have been successfully modeled by solving the Ornstein-Zernike equation with various closures including the mean spherical approximation (MSA) [1] and the hypernetted chain (HNC) approximation [2]. In inhomogeneous hard-sphere systems, density functional theory (DFT) has been applied to both uncharged (see Refs. [3,4], for example) and charged (see Refs. [5–8], for example) hard-sphere fluids.

DFT determines thermodynamic properties of inhomogeneous fluids from the excess free energy F_{ex} and its functional dependence on the set of all the particle densities $\{\rho_k(\mathbf{y})\}$:

$$F_{\text{ex}} = F_{\text{ex}}[\{\rho_k(\mathbf{y})\}]. \quad (1)$$

We decompose F_{ex} into two terms, namely the hard-sphere (HS) and electrostatic (ES) excess free energy functionals, so that

$$F_{\text{ES}}[\{\rho_k(\mathbf{y})\}] = F_{\text{ex}}[\{\rho_k(\mathbf{y})\}] - F_{\text{HS}}[\{\rho_k(\mathbf{y})\}]. \quad (2)$$

Various formulations of the HS functional F_{HS} exist [9], including Rosenfeld's [10] and improved formulations based on it [11–13]. On the other hand, a first-principles formulation of the ES functional is not known, although several ap-

proximations exist [5,11,14]. (Mier-y-Teran *et al.* [5] give an overview of other approximations.) Although Monte Carlo (MC) methods can simulate charged systems, they are limited to equilibrium systems (cf. Refs. [15,16]) and relatively high ion densities. Furthermore, because of the vast difference in computation time between MC and DFT methods, MC simulations sample a much smaller parameter space than DFT methods. Of course, MC simulations are invaluable to compare the approximate DFT results against a system with less restrictive approximations.

One approximation of the ES functional, introduced by Rosenfeld, is based on the perturbation of a bulk (homogeneous) reference fluid [11]. This formulation of the functional has been applied to several inhomogeneous systems [7,8]. However, not all systems are amenable to perturbation around a bulk fluid; implicit in any perturbation approximation is the expectation that the final results should be a small correction to the reference (unperturbed) system. If the particle densities vary by large amounts within the system, then the bulk-fluid perturbation ansatz probably will not work. Moreover, such large density variations occur in many systems of interest, especially biological ones; active sites of proteins are often highly charged, attracting high concentrations of counter charge [17]. One example is the *L*-type calcium ion channel whose pore wall contains four negatively charged amino acids in a ring [18]. Inside the channel the Ca^{2+} concentration is tens of molar, while in the baths surrounding the channel it is of the order of $10^{-6}M$ [16,19].

To describe such electrolyte systems, we recently proposed a version of the ES functional that replaces Rosenfeld's spatially uniform reference fluid with a location-dependent reference fluid [16]. In addition, the inhomogeneous reference fluid densities were computed

*Email address: dirk_gillespie@rush.edu

†Email address: wnonner@chroma.med.miami.edu

‡Email address: beisenbe@rush.edu

from the densities produced by the previous calculation and iterated to self-consistency. The numerical results compared well to MC simulations (Figs. 2 and 3 of Ref. [16]).

In this paper, we reformulate this iterative method (Sec. II) into a new ES functional using the key idea that iteratively updating the reference fluid is equivalent to making the “reference” fluid densities into functionals of the fluid densities (the RFD functional). This new functional dependence is the basis for the ES functional F_{ES} (Sec. III). The first-order ES direct correlation function (DCF) $c_i^{(1),\text{ES}}$ resulting from this ES excess free energy is discussed in Sec. IV. The functional differentiation that yields $c_i^{(1),\text{ES}}$ includes terms that arise because the reference densities are functionals of the densities. These terms were not considered in our previous work [16]. We show that these terms cancel exactly and therefore the previously described iteration method and the new ES functional are, in fact, mathematically equivalent (Appendix B). One further consequence of this analysis is that the problem of finding an accurate ES functional is reduced to finding a suitable RFD functional (Sec. IV). Finally, we discuss one possible form for the RFD functional (Sec. V) and analyze the strengths and weaknesses of this ES functional (Sec. VI).

II. INHOMOGENEOUS REFERENCE FLUID AND ITERATION

In Ref. [16] we proposed an ES functional based on perturbation of an inhomogeneous reference fluid. This generalization of Rosenfeld’s method [11] expands the ES functional $F_{\text{ES}}[\{\rho_k(\mathbf{y})\}]$ in a functional Taylor series in powers of

$$\Delta\rho_i(\mathbf{x}) = \rho_i(\mathbf{x}) - \rho_i^{\text{ref}}(\mathbf{x}), \quad (3)$$

where $\rho_i^{\text{ref}}(\mathbf{x})$ is a given inhomogeneous reference density profile. The original derivation [11] used homogeneous reference fluid densities for which $\rho_i^{\text{ref}}(\mathbf{x})$ is independent of \mathbf{x} .

Following Rosenfeld, we truncate after the quadratic term:

$$\begin{aligned} F_{\text{ES}}[\{\rho_k(\mathbf{y})\}] &\approx F_{\text{ES}}[\{\rho_k^{\text{ref}}(\mathbf{y})\}] - kT \\ &\times \sum_i \int c_i^{(1),\text{ES}}[\{\rho_k^{\text{ref}}(\mathbf{y})\}; \mathbf{x}] \Delta\rho_i(\mathbf{x}) d\mathbf{x} \\ &- \frac{kT}{2} \sum_{i,j} \int \int c_{ij}^{(2),\text{ES}}[\{\rho_k^{\text{ref}}(\mathbf{y})\}; \mathbf{x}, \mathbf{x}'] \\ &\times \Delta\rho_i(\mathbf{x}) \Delta\rho_j(\mathbf{x}') d\mathbf{x} d\mathbf{x}', \end{aligned} \quad (4)$$

where $c_i^{(1),\text{ES}}[\{\rho_k^{\text{ref}}(\mathbf{y})\}; \mathbf{x}]$ and $c_{ij}^{(2),\text{ES}}[\{\rho_k^{\text{ref}}(\mathbf{y})\}; \mathbf{x}, \mathbf{x}']$ are the ES components (that is, they exclude the HS components) of the first- and second-order DCFs, respectively, of the reference fluid. The relation

$$c_i^{(1),\text{ES}}[\{\rho_k(\mathbf{y})\}; \mathbf{x}] = -\frac{1}{kT} \frac{\delta F_{\text{ES}}}{\delta \rho_i(\mathbf{x})} \quad (5)$$

implies that

$$\begin{aligned} c_i^{(1),\text{ES}}[\{\rho_k(\mathbf{y})\}; \mathbf{x}] &\approx c_i^{(1),\text{ES}}[\{\rho_k^{\text{ref}}(\mathbf{y})\}; \mathbf{x}] \\ &+ \sum_j \int c_{ij}^{(2),\text{ES}}[\{\rho_k^{\text{ref}}(\mathbf{y})\}; \mathbf{x}, \mathbf{x}'] \\ &\times \Delta\rho_j(\mathbf{x}') d\mathbf{x}'. \end{aligned} \quad (6)$$

The notation $c_i^{(1),\text{ES}}[\{\rho_k(\mathbf{y})\}; \mathbf{x}]$ (following Rosenfeld [11]) is used to indicate explicitly that $c_i^{(1),\text{ES}}$ is a function of \mathbf{x} and that, at every location \mathbf{x} , it is also a functional of the densities $\{\rho_k(\mathbf{y})\}$. Similar notation is used for $c_{ij}^{(2),\text{ES}}[\{\rho_k^{\text{ref}}(\mathbf{y})\}; \mathbf{x}, \mathbf{x}']$.

Next we discuss general aspects of the functional, leaving the details of estimating $c_i^{(1),\text{ES}}[\{\rho_k^{\text{ref}}(\mathbf{y})\}; \mathbf{x}]$ and $c_{ij}^{(2),\text{ES}}[\{\rho_k^{\text{ref}}(\mathbf{y})\}; \mathbf{x}, \mathbf{x}']$ for a given inhomogeneous reference fluid until Sec. V.

Equation (6) is the first-order ES DCF we used to compute the output densities $\rho_i(\mathbf{x})$ in Ref. [16]. In that paper, the final fluid densities were determined by iteratively updating the reference fluid densities $\rho_k^{\text{ref}}(\mathbf{y})$: an initial guess for the densities $\rho_i(\mathbf{x})$ was chosen and an initial set of reference fluid densities $\rho_k^{\text{ref}}(\mathbf{y})$ was calculated (Sec. V) and used in Eq. (6) to compute a new set of output densities $\rho_i(\mathbf{x})$; these, in turn, were used to compute the next set of reference fluid densities $\rho_k^{\text{ref}}(\mathbf{y})$. This cycle was continued until there was no significant change in the output densities $\rho_i(\mathbf{x})$.

We illustrate this procedure for the inhomogeneous reference fluid with an example developed in Ref. [16]. Consider two large compartments: the left compartment contains a fluid of $6M$ Ca^{2+} and $24M$ anions with valence $-1/2$ (denote them $A^{1/2-}$); the right compartment contains $0.1M$ CaCl_2 . These two compartments are brought into contact and allowed to equilibrate with the restriction that $A^{1/2-}$ are confined to the left compartment with a hard-wall potential; Ca^{2+} and Cl^- are allowed to equilibrate throughout both compartments. A discussion of the valence $-1/2$ species and specific details of the system are given in Appendix A.

In Figs. 1 and 2 the DFT results are compared to MC simulations. Figure 1(a) shows the output Ca^{2+} concentration for each of the four different Ca^{2+} reference fluid concentrations shown in Fig. 1(b). Figure 2 shows these concentrations for $A^{1/2-}$. To compare our results to the bulk-fluid reference method, we choose for the initial reference fluid the bulk fluid of the right compartment. The results for this case [dot-dashed line in Figs. 1(a) and 2(a)] are poor because (i) the large differences between the output and reference densities challenge the perturbation ansatz in this situation and (ii) the MSA is used to estimate the second-order ES DCF in Eq. (6) (Sec. V). These sources of error will be discussed in detail in Sec. VI B. The effect of these errors is an inaccurate calculation of the first-order ES DCF in the far left compartment. Thus, in this grand canonical ensemble, the resulting inaccurately computed concentrations in that bath do not reach the $24M$ and $6M$ levels for $A^{1/2-}$ and Ca^{2+} , respectively [dot-dashed line in Figs. 1(a) and 2(a)]. Although we do not show them, similar inaccuracies were

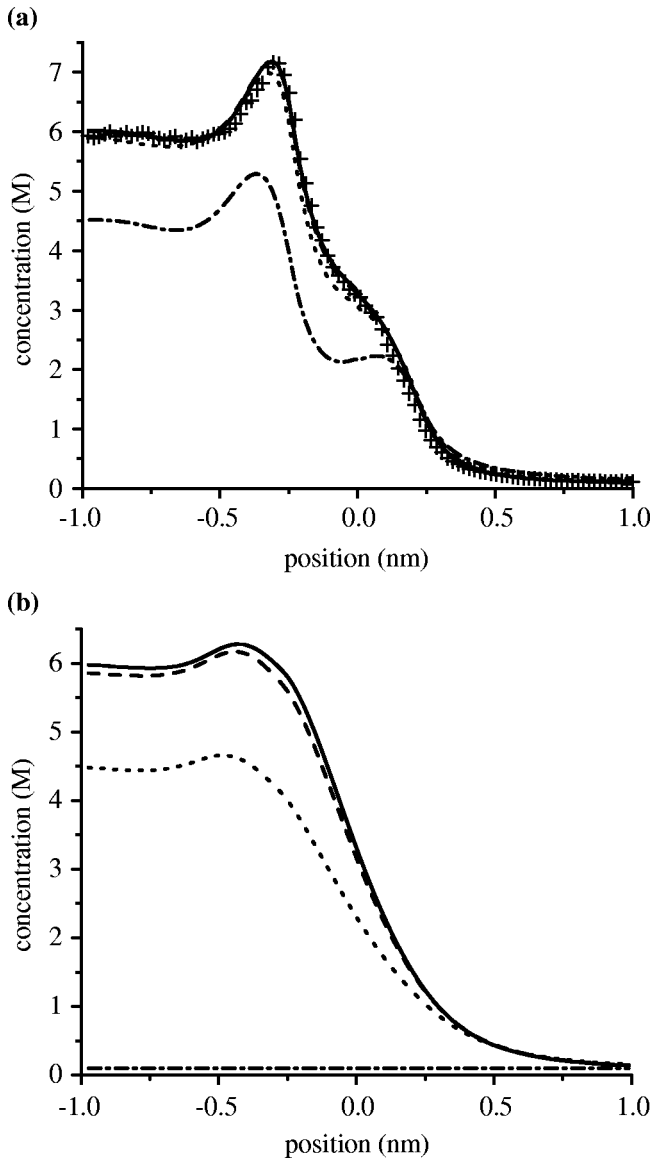


FIG. 1. Electrical double layer at the interface of two electrolyte compartments described in Appendix A. Panel (a) shows the four concentration profiles of Ca^{2+} calculated from the corresponding Ca^{2+} reference fluid concentrations shown in panel (b). The curves converge to the final solution (solid line) in three iterations. In panel (a) the symbols are the results of Monte Carlo simulations. The curves in panel (b) are initial reference concentration (dot-dashed line); first iterative refinement (short-dashed line) calculated using output concentrations of the previous computation [dot-dash curve in panel (a)] using Eq. (16); second iterative refinement (long-dashed line) calculated using the short-dash curve in panel (a); third (and final) iterative refinement (solid) calculated using the long-dash curve in panel (a).

found when we chose the bulk reference fluid densities to be $24M A^{1/2-}$, $6M \text{Ca}^{2+}$, and $0M \text{Cl}^-$, the densities in the far left compartment.

The errors are substantially reduced when iteration is used to successively revise the reference fluid densities. Figures 1(a) and 2(a) show substantial improvement in just one iteration (short-dashed lines), with $A^{1/2-}$ having almost con-

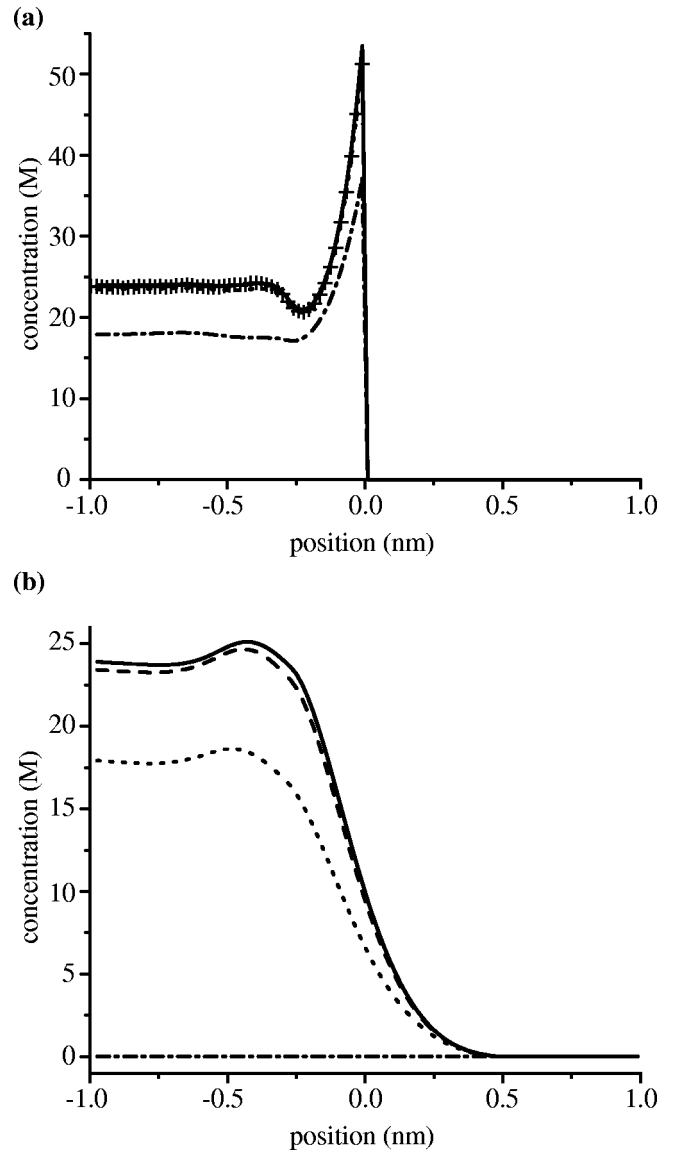


FIG. 2. Same as Fig. 1 except that in panel (a) are the output concentrations of $A^{1/2-}$ and in panel (b) are their reference fluid concentration of $A^{1/2-}$.

verged to its final concentration profile. While Ca^{2+} requires more iterations, still only two or three iterations are needed to reach stable output concentrations. In this example, using reference fluid densities that depend on the output densities yields accurate results whereas the bulk-fluid reference method fails.

In all the inhomogeneous systems we have studied so far, the computed densities converge to their final values in three iterations or less [16,20].

III. ELECTROSTATIC FUNCTIONAL

In perturbation theory, a reference (unperturbed) system, by definition, does not depend on the final, output variables. At each step of the iteration in the preceding section, such a fixed reference fluid is used to calculate fluid densities. However, the iteration cycle taken as a whole makes the reference

fluid densities $\rho_k^{\text{ref}}(\mathbf{y})$ depend on the densities $\rho_i(\mathbf{x})$. In this view, the reference fluid *per se* no longer exists. In the case we consider here, at each location \mathbf{y} , every $\rho_k^{\text{ref}}(\mathbf{y})$ is made a functional of all $\rho_i(\mathbf{x})$:

$$\rho_k^{\text{ref}}(\mathbf{y}) = \bar{\rho}_k[\{\rho_i(\mathbf{x})\}; \mathbf{y}]. \quad (7)$$

We call $\bar{\rho}_k[\{\rho_i(\mathbf{x})\}; \mathbf{y}]$ the RFD functional, recalling its origin as the ‘‘reference fluid density’’ functional. However, strictly speaking, this functional eliminates the concept of the reference fluid entirely.

The ES functional (4) may then be written as

$$F_{\text{ES}}[\{\rho_k(\mathbf{y})\}] \approx F_{\text{ES}}[\{\bar{\rho}_k(\mathbf{y})\}] + F_{\text{ES}}^{(1)}[\{\bar{\rho}_k(\mathbf{y})\}, \{\rho_k(\mathbf{y})\}] + F_{\text{ES}}^{(2)}[\{\bar{\rho}_k(\mathbf{y})\}, \{\rho_k(\mathbf{y})\}], \quad (8)$$

where $F_{\text{ES}}[\{\bar{\rho}_k(\mathbf{y})\}]$ is the ES excess free energy of a fluid with densities $\{\bar{\rho}_k(\mathbf{y})\}$,

$$-\frac{1}{kT} F_{\text{ES}}^{(1)}[\{\bar{\rho}_k(\mathbf{y})\}, \{\rho_k(\mathbf{y})\}] = \sum_i \int \bar{c}_i^{(1),\text{ES}}(\mathbf{x}) \Delta \rho_i(\mathbf{x}) d\mathbf{x} \quad (9)$$

and

$$-\frac{1}{kT} F_{\text{ES}}^{(2)}[\{\bar{\rho}_k(\mathbf{y})\}, \{\rho_k(\mathbf{y})\}] = \frac{1}{2} \sum_{i,j} \int \int \bar{c}_{ij}^{(2),\text{ES}}(\mathbf{x}, \mathbf{x}') \Delta \rho_i(\mathbf{x}) \Delta \rho_j(\mathbf{x}') d\mathbf{x} d\mathbf{x}', \quad (10)$$

with

$$\Delta \rho_k(\mathbf{x}) = \rho_k(\mathbf{x}) - \bar{\rho}_k(\mathbf{x}), \quad (11)$$

$$\bar{c}_i^{(1),\text{ES}}(\mathbf{x}) = c_i^{(1),\text{ES}}[\{\bar{\rho}_k(\mathbf{y})\}; \mathbf{x}] = -\frac{1}{kT} \frac{\delta F_{\text{ES}}[\{\bar{\rho}_k(\mathbf{y})\}]}{\delta \bar{\rho}_i(\mathbf{x})}, \quad (12)$$

and

$$\begin{aligned} \bar{c}_{ij}^{(2),\text{ES}}(\mathbf{x}, \mathbf{x}') &= c_{ij}^{(2),\text{ES}}[\{\bar{\rho}_k(\mathbf{y})\}; \mathbf{x}, \mathbf{x}'] \\ &= -\frac{1}{kT} \frac{\delta^2 F_{\text{ES}}[\{\bar{\rho}_k(\mathbf{y})\}]}{\delta \bar{\rho}_i(\mathbf{x}) \delta \bar{\rho}_j(\mathbf{x}')}. \end{aligned} \quad (13)$$

The RFD functional $\bar{\rho}_k[\{\rho_i(\mathbf{x})\}; \mathbf{y}]$ remains to be specified. One possible choice is a given and fixed reference fluid, as in the Rosenfeld bulk-reference method, whereas another possibility involving nonlocal $\bar{\rho}_k(\mathbf{y})$ is given in Sec. V. Properties that the RFD functional must satisfy are given in Sec. VI A.

IV. FIRST-ORDER DIRECT CORRELATION FUNCTION

Because of the technical nature of the derivation of the first-order ES DCF, it is presented in Appendix B. Here we merely state the result

$$c_i^{(1),\text{ES}}(\mathbf{x}) \approx \bar{c}_i^{(1),\text{ES}}(\mathbf{x}) + \sum_j \int \bar{c}_{ij}^{(2),\text{ES}}(\mathbf{x}, \mathbf{x}') \Delta \rho_j(\mathbf{x}') d\mathbf{x}', \quad (14)$$

where

$$\Delta \rho_k(\mathbf{x}) = \rho_k(\mathbf{x}) - \bar{\rho}_k(\mathbf{x}). \quad (15)$$

Comparing this to the formulation for a given and fixed set of reference densities $\{\bar{\rho}_k(\mathbf{x})\}$ [Eq. (6)] shows that these two formulations are identical; that is, *the formula used to compute the first-order ES DCF is the same for any choice of RFD functional $\bar{\rho}_k(\mathbf{x})$* . Of course, different *specific* choices of RFD functionals will give different functions $c_i^{(1),\text{ES}}(\mathbf{x})$, but the formula [that is, the dependence on the $\bar{\rho}_k(\mathbf{x})$] is the same. The problem remaining to be solved is finding a RFD functional that accurately estimates the first-order ES DCF of the fluid being studied.

V. RFD FUNCTIONAL: ONE POSSIBLE CHOICE

In this section we describe one possible choice for the RFD functional. Beyond choosing a RFD functional, however, the first- and second-order ES DCFs of the fluid with densities $\bar{\rho}_i(\mathbf{x})$ must also be calculated. We do this by taking advantage of the idea that *the fluid with densities $\bar{\rho}_i(\mathbf{x})$ does not have to be a physically real fluid*; the functional $\bar{\rho}_i[\{\rho_k(\mathbf{x}')\}; \mathbf{x}]$ is a mathematical construction that one is free to choose so that the required DCFs can be calculated. This is opposite of the overall problem being solved: to minimize the free energy of the system, the fluid densities $\rho_i(\mathbf{x})$ of the system are determined from $c_i^{(1),\text{ES}}(\mathbf{x})$ and the other components of the chemical potential; on the other hand, to calculate $c_i^{(1),\text{ES}}(\mathbf{x})$ with Eq. (14), we *choose* $\bar{\rho}_i(\mathbf{x})$ in such a way that $\bar{c}_i^{(1),\text{ES}}(\mathbf{x})$ and $\bar{c}_{ij}^{(2),\text{ES}}(\mathbf{x}, \mathbf{x}')$ can be approximated.

To illustrate this, we use the new functional dependence (7) to recast the iterative updating of the reference fluid of Sec. II and Ref. [16] into a specific choice of the RFD functional $\bar{\rho}_i[\{\rho_k(\mathbf{x}')\}; \mathbf{x}]$. We define

$$\bar{\rho}_i[\{\rho_k(\mathbf{x}')\}; \mathbf{x}] = \int \alpha_i(\mathbf{x}') \rho_i(\mathbf{x}') w(\mathbf{x}', \mathbf{x}) d\mathbf{x}', \quad (16)$$

where, if $z_i \geq 0$ (where z_i is the valence of ion species i),

$$\alpha_i(\mathbf{x}) = A(\mathbf{x}) \quad (17)$$

and, if $z_i < 0$,

$$\alpha_i(\mathbf{x}) = A(\mathbf{x}) B(\mathbf{x}), \quad (18)$$

with

$$A(\mathbf{x}) = \frac{\sum_k z_k^2 \rho_k(\mathbf{x})}{\sum_{z_k \geq 0} z_k^2 \rho_k(\mathbf{x}) + B(\mathbf{x}) \sum_{z_k < 0} z_k^2 \rho_k(\mathbf{x})} \quad (19)$$

and

$$B(\mathbf{x}) = \frac{\sum_{z_k \geq 0} z_k \rho_k(\mathbf{x})}{\sum_{z_k < 0} |z_k| \rho_k(\mathbf{x})}. \quad (20)$$

This choice of scaling factor $\alpha_i(\mathbf{x})$ ensures that the fluid with densities $\{\alpha_i(\mathbf{x})\rho_i(\mathbf{x})\}$ is charge neutral and has the same ionic strength at every point \mathbf{x} as the fluid with densities $\{\rho_i(\mathbf{x})\}$. The weight function $w(\mathbf{x}', \mathbf{x})$ is given by

$$w(\mathbf{x}', \mathbf{x}) = \frac{\theta(|\mathbf{x}' - \mathbf{x}| - R_{\text{ES}}(\mathbf{x}))}{\frac{4\pi}{3} R_{\text{ES}}^3(\mathbf{x})}, \quad (21)$$

where θ is the unit step function [that is, $\theta(x > 0) = 0$ and $\theta(x \leq 0) = 1$]. The radius of the sphere $R_{\text{ES}}(\mathbf{x})$ over which we average is the local electrostatic length scale. ‘‘Length scale’’ is not a well-defined quantity and we approximate it as the sum of average ion radii R_k and the local screening length $s(\mathbf{x})$:

$$R_{\text{ES}}(\mathbf{x}) \approx \frac{\sum_k \alpha_k(\mathbf{x}) \rho_k(\mathbf{x}) R_k}{\sum_k \alpha_k(\mathbf{x}) \rho_k(\mathbf{x})} + s(\mathbf{x}). \quad (22)$$

To estimate the first-order ES DCF $\bar{c}_i^{(1),\text{ES}}(\mathbf{x})$ at each point, we use a bulk formulation (specifically the MSA) at each point \mathbf{x} with densities $\bar{\rho}_k(\mathbf{x})$. Similarly, for the second-order ES DCF $\bar{c}_{ij}^{(2),\text{ES}}(\mathbf{x}, \mathbf{x}')$ we use an approximation of the MSA ES DCF [21] due to Blum and Rosenfeld [7,22]. *This use of the bulk correlation functions at each point \mathbf{x} is why the densities $\bar{\rho}_k(\mathbf{x})$ were made locally charge neutral.* In general, the densities $\bar{\rho}_k(\mathbf{x})$ do not have to be charge neutral everywhere, as long as these densities can be chosen so that the first- and second-order ES DCFs can be approximated for all \mathbf{x} .

The MSA bulk formulation also allows estimation of the screening length by using the MSA screening length $1/2\Gamma$ at each point with densities $\{\bar{\rho}_k(\mathbf{x})\}$:

$$s(\mathbf{x}) = \frac{1}{2\Gamma(\mathbf{x})}. \quad (23)$$

Thus the screening length depends on the densities $\bar{\rho}_k(\mathbf{x})$ which, in turn, depend on the screening length; at every point \mathbf{x} the screening length $1/2\Gamma$ used to calculate $\bar{\rho}_k(\mathbf{x})$ must equal the screening length $1/2\Gamma$ calculated from $\bar{\rho}_k(\mathbf{x})$. For

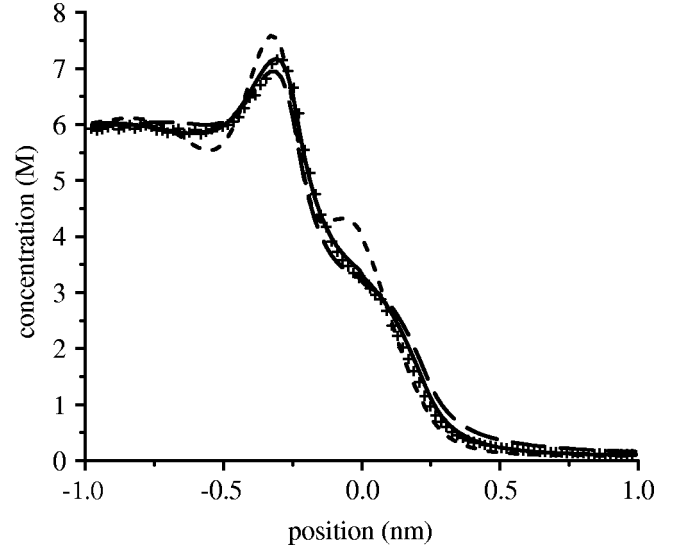


FIG. 3. The effect of using different length scales in the RFD functional (16) on calculated fluid concentrations: $\frac{1}{2}R_{\text{ES}}(\mathbf{x})$ (short-dashed line), $R_{\text{ES}}(\mathbf{x})$ (solid line), and $2R_{\text{ES}}(\mathbf{x})$ (long-dashed line), where $R_{\text{ES}}(\mathbf{x})$ is defined in Eq. (22). The symbols are the results of MC simulations.

each \mathbf{x} , this equality is a one-dimensional algebraic equation in Γ which may be solved by iteration [16], although other algorithms for root finding are significantly more efficient [23]. In this paper, we used Brent’s method for such calculations [23].

We estimate the input ES DCFs with the MSA because the MSA gives analytic results for both the first-order DCF (excess chemical potential) [1] and the second-order DCF [21,22]. Other bulk formulations such as the HNC or test-particle self-consistent method [11] could be used instead and may yield better results. However, even with other bulk theories, we note that one can still approximate the ES length scale R_{ES} with the same MSA screening length formulation used here. Because the value of R_{ES} used to average the densities $\rho_k(\mathbf{x}')$ ranges (approximately) from 0.1 to 1 nm or more, small differences in R_{ES} from different calculation methods have little effect on the averaged densities $\bar{\rho}_i(\mathbf{x})$. Furthermore, the calculation of R_{ES} with the MSA screening length is straightforward and computationally efficient, as described above.

While small differences in R_{ES} do not result in significant differences in fluid densities, the choice of $R_{\text{ES}}(\mathbf{x})$ is important. For instance, using $\frac{1}{2}R_{\text{ES}}(\mathbf{x})$ or $2R_{\text{ES}}(\mathbf{x})$ in the example of Sec. II gives different answers. As shown in Fig. 3, neither function captures the length scale of the Ca^{2+} concentration as well as the original definition of $R_{\text{ES}}(\mathbf{x})$ in Eq. (22): the Ca^{2+} concentration calculated from $2R_{\text{ES}}(\mathbf{x})$ decays to the bulk densities away from the interface too slowly; the concentration calculated from $\frac{1}{2}R_{\text{ES}}(\mathbf{x})$ has a density peak that is too large, resulting in spurious HS packing effects. In both cases $\Delta\rho_k(\mathbf{x}')$ are larger than when the concentration is calculated from $R_{\text{ES}}(\mathbf{x})$. When $\frac{1}{2}R_{\text{ES}}(\mathbf{x})$ is used, $\bar{\rho}_i(\mathbf{x})$ are less smooth so that the pointwise application of the MSA theory is less accurate.

We have also reversed the two steps in the calculation of $\bar{\rho}_k(\mathbf{x})$, this time first individually averaging $\rho_k(\mathbf{x}')$ over the sphere of radius $R_k + s(\mathbf{x})$ and then computing $\bar{\rho}_k(\mathbf{x})$ by enforcing local charge neutrality and preserving local ionic strength. The results were similar to those shown in Figs. 1(a) and 2(a).

Finally, we note that there is an infinite number of ways to make $\bar{\rho}_i(\mathbf{x})$ charge neutral (although, in general, they are not required to be). We choose the scaling factor $\alpha_i(\mathbf{x})$ in Eq. (16) because it is the simplest choice that changes both cation and anion densities. By scaling all the cation densities with one factor and all the anions with another factor, the problem of charge neutrality simplifies to solving two coupled equations for two unknowns (A and B) at each point \mathbf{x} . This can be solved analytically when retaining the same ionic strength at each \mathbf{x} .

VI. DISCUSSION

In this paper, we propose an improved formulation of the ES free energy functional F_{ES} [Eq. (8)] based on the work of Ref. [16]. The functional generalizes Rosenfeld's perturbation of a bulk reference fluid [11] by including a new functional dependence [the RFD functional of Eq. (7)] that eliminates the concept of a fixed reference fluid altogether. Even with the addition of the RFD functional $\bar{\rho}_i[\{\rho_k(\mathbf{x}')\};\mathbf{x}]$, the first-order ES DCF formula [Eq. (14)] does not become more complex than Rosenfeld's formula [11] because all additional terms due to the RFD functional cancel (Appendix B). Thus, Rosenfeld's perturbation approach to computing the first-order ES DCF is more general than the original derivation would imply: if the functional dependence of F_{ES} on $\rho_i(\mathbf{x})$ and $\bar{\rho}_i(\mathbf{x})$ is given by Eq. (8), then $c_i^{(1),\text{ES}}(\mathbf{x})$ is given by Eq. (14) for *any* choice of the RFD functional $\bar{\rho}_i[\{\rho_k(\mathbf{x}')\};\mathbf{x}]$. Since different *specific* choices of the RFD functional will yield different ES free energies and first-order ES DCFs, the problem of finding the ES free energy functional that correctly describes a system is essentially reduced to finding a reasonable RFD functional. Furthermore, this search is greatly simplified by the following observations: (1) evaluating a new RFD functionals requires only a substitution into Eq. (14) to determine the first-order ES DCF; (2) the RFD functional may be evaluated numerically since no functional derivatives of the RFD functional are required to compute the first-order ES DCF; (3) if fluid densities $\rho_i(\mathbf{x})$ can be determined for a given set of densities $\{\bar{\rho}_i(\mathbf{x})\}$, $\bar{c}_i^{(1),\text{ES}}(\mathbf{x})$, and $\bar{c}_{ij}^{(2),\text{ES}}(\mathbf{x},\mathbf{x}')$, then the problem can be solved iteratively as in Ref. [16] (reviewed in Sec. II) by updating $\{\bar{\rho}_i(\mathbf{x})\}$, $\bar{c}_i^{(1),\text{ES}}(\mathbf{x})$, and $\bar{c}_{ij}^{(2),\text{ES}}(\mathbf{x},\mathbf{x}')$.

A. The RFD functional

Equation (14) is, in principle, valid for any choice of densities $\bar{\rho}_i(\mathbf{x})$. While there are no *a priori* constraints on the RFD functional $\bar{\rho}_i[\{\rho_k(\mathbf{x}')\};\mathbf{x}]$ that may be used in Eq. (14), there are important practical considerations in choosing a RFD functional that yields an accurate F_{ES} : $\Delta\rho_k(\mathbf{x}')$ must

be small throughout the system and, for the fluid with densities $\{\bar{\rho}_i(\mathbf{x})\}$, one must be able to calculate (either analytically or numerically) both the first- and second-order DCFs $\bar{c}_i^{(1),\text{ES}}(\mathbf{x})$ and $\bar{c}_{ij}^{(2),\text{ES}}(\mathbf{x},\mathbf{x}')$.

This may seem more difficult than the original problem where, to determine the structure of an inhomogeneous fluid in equilibrium, only the first-order DCF needs to be determined; now one must also compute a second-order DCF. However, unlike the actual fluid densities $\rho_k(\mathbf{x}')$, the densities $\bar{\rho}_i(\mathbf{x})$ can be *chosen* so that one can approximate both the DCFs $\bar{c}_i^{(1),\text{ES}}(\mathbf{x})$ and $\bar{c}_{ij}^{(2),\text{ES}}(\mathbf{x},\mathbf{x}')$; $\bar{\rho}_i(\mathbf{x})$ are not required to represent a physically real fluid. For example, the specific functional form of $\bar{\rho}_i[\{\rho_k(\mathbf{x}')\};\mathbf{x}]$ we adopt in Eq. (16) is an average of local densities $\rho_k(\mathbf{x}')$ over a sphere with radius equal to the ES length scale R_{ES} . In practice, R_{ES} extends (approximately) from 0.1 to 1 nm (or more) beyond the ion radius, depending on the local screening length [Eq. (22)]. Thus, the densities $\bar{\rho}_i(\mathbf{x})$ are nonlocal and average out local variations in density; $\bar{\rho}_i(\mathbf{x})$ vary smoothly and slowly, even if the local densities $\rho_k(\mathbf{x}')$ do not [compare Figs. 2(a) and 2(b)]. Since $\bar{\rho}_i(\mathbf{x})$ were also made charge neutral, it follows that the ES DCFs $\bar{c}_i^{(1),\text{ES}}(\mathbf{x})$ and $\bar{c}_{ij}^{(2),\text{ES}}(\mathbf{x},\mathbf{x}')$ may be approximated (at least to first order) by their local bulk values.

A shortcoming of the nonlocal densities $\bar{\rho}_i(\mathbf{x})$ defined in Eq. (16) is that they do not follow fluid density peaks that are more narrow than R_{ES} , the length scale of the averaging [compare Figs. 2(a) and 2(b)]. In such regions, $\Delta\rho_k(\mathbf{x}')$ will *not* be small. In the cases we have considered (Figs. 1 and 2, and Refs. [16,20]), density peaks are still accurately computed because the *total* chemical potential is dominated by its other components (especially the HS and electrostatic mean-field components).

On the other hand, the RFD functional described in Sec. V seems to succeed because it tends to keep $\Delta\rho_k(\mathbf{x}')$ small. In the example of Figs. 1 and 2, it is correct in the both compartments far from the interface. Moreover, near the interface, the RFD densities $\bar{\rho}_k(\mathbf{y})$ have the correct length scale to make $\Delta\rho_k(\mathbf{x}')$ small, especially for Ca^{2+} [compare Figs. 1(a) and 1(b)].

B. Sources of error

As discussed previously, an important source of error in the ES functional (8) is the size of the perturbation [that is, $\Delta\rho_k(\mathbf{x}')$]. Other sources of error are the inputs to the functional, specifically the formulas used to estimate the first- and second-order DCFs $\bar{c}_i^{(1),\text{ES}}(\mathbf{x})$ and $\bar{c}_{ij}^{(2),\text{ES}}(\mathbf{x},\mathbf{x}')$. In our calculations, we use the MSA to estimate both of these quantities. While the deficiencies of the MSA are well known [24], the choice of the MSA is especially problematic for the second-order ES DCF, as we briefly demonstrate.

Consider the case when both the fluid and reference fluid densities are *uniform* and the ions have the same radius R [the restricted primitive model (RPM)]. In the RPM, the MSA second-order ES DCF is [1]

$$kT\bar{c}_{ij}^{(2),\text{ES}}(\mathbf{x},\mathbf{x}') \approx -\frac{z_i z_j e^2}{4\pi\epsilon\epsilon_0} \left(\frac{B}{R} - \frac{B^2}{4R^2} |\mathbf{x}-\mathbf{x}'| \right) \quad (24)$$

if $|\mathbf{x}-\mathbf{x}'| < 2R$ and

$$kT\bar{c}_{ij}^{(2),\text{ES}}(\mathbf{x},\mathbf{x}') \approx -\frac{z_i z_j e^2}{4\pi\epsilon\epsilon_0} \frac{1}{|\mathbf{x}-\mathbf{x}'|} \quad (25)$$

otherwise. Here,

$$B = \frac{x+1-\sqrt{1+2x}}{x}, \quad (26)$$

where

$$x^2 = \frac{4R^2 e^2}{kT\epsilon\epsilon_0} \sum_k z_k^2 \bar{\rho}_k. \quad (27)$$

From this it follows that the perturbation term for the first-order ES DCF is identically zero if $\Delta\rho_j(\mathbf{x}')$ is constant (and nonzero):

$$\sum_j \int \bar{c}_{ij}^{(2),\text{ES}}(\mathbf{x},\mathbf{x}') \Delta\rho_j(\mathbf{x}') d\mathbf{x}' = 0. \quad (28)$$

This means that the computed first-order ES DCF [Eq. (14)] is that of the reference fluid. Therefore, even in this very simple case, it is not possible to correctly compute the first-order ES DCF using the MSA second-order ES DCF. Furthermore, when the ions are of different size, the perturbation term remains small (although not necessarily identically zero) when $\Delta\rho_j(\mathbf{x}')$ is constant. This correlation function error is one source of the discrepancies in the left-compartment results in the initial calculations of Figs. 1(a) and 2(a) (dot-dashed lines).

The contribution of this correlation function error can, however, be controlled by choosing a RFD functional that minimizes $\Delta\rho_j(\mathbf{x}')$. For such a RFD functional, the perturbation term is minimal and therefore so is the correlation function error. Furthermore, in the limit of uniform densities (as considered in this section), $\Delta\rho_j(\mathbf{x}')=0$ for such a RFD functional and the first-order ES DCF is computed correctly by the bulk formulation. This is illustrated in Figs. 1 and 2 (Sec. II) where $\bar{\rho}_k(\mathbf{x}')$ in the far left compartment converge to the final fluid densities (solid lines).

Thus both major sources of errors are minimized when the RFD functional is chosen to make $\Delta\rho_j(\mathbf{x}')$ as small as possible.

Like many others [5–8], we use the MSA formulation because of its analytic results and because the overall results of the DFT calculations compare well to MC results (Figs. 1 and 2, and Refs. [16,20]). We describe some of the problems with using this particular correlation function not only because one must be aware of these, but also to show how the ES functional (8) overcomes these problems. Other, more accurate, bulk formulations should also be investigated.

C. Generalizations of the method

It was recently pointed out to us by Roth [25] that the method described in this paper and the ES functional (8) is more general than was originally intended: it can be applied to systems with particle-particle interactions other than Coulombic (for example, Yukawa or square well). This can be seen by noting that the derivation of the ES functional (8) does not assume any specific particle-particle interaction potential (except that it is something in addition to HS). Therefore it is not until the RFD functional $\bar{\rho}_i[\{\rho_k(\mathbf{x}')\};\mathbf{x}]$ and the corresponding DCFs $\bar{c}_i^{(1),\text{ES}}(\mathbf{x})$ and $\bar{c}_{ij}^{(2),\text{ES}}(\mathbf{x},\mathbf{x}')$ are chosen, that the interaction potential must be specified. (Note that the RFD functional described in Sec. V *does* depend on the interaction potential.) Since the interaction potential does not appear anywhere else in the theory, the inhomogeneous fluid described by the excess free energy (8) is the fluid with the particle-particle interaction potential used to compute $\bar{c}_i^{(1),\text{ES}}(\mathbf{x})$ and $\bar{c}_{ij}^{(2),\text{ES}}(\mathbf{x},\mathbf{x}')$.

VII. CONCLUSION

We have shown that the ES functional (8) is a starting point for computing the first-order ES DCF for any choice of RFD functional $\bar{\rho}_i[\{\rho_k(\mathbf{x}')\};\mathbf{x}]$ [Eq. (7)]. The specific choice of RFD functional discussed in Sec. V works well when combined with first- and second-order ES DCFs computed from point-by-point applications of the MSA. Furthermore, this RFD functional reduces the two largest sources of error by keeping $\Delta\rho_k(\mathbf{x}')$ small throughout the system. This preserves the perturbation ansatz while at the same time minimizing the effects of using a poor input correlation function in the perturbation term in Eq. (14).

For charged, hard-sphere fluids, this work may be extended by using bulk formulations other than the MSA or using other RFD functionals for which the first- and second-order ES DCFs can be computed.

ACKNOWLEDGMENTS

We are most grateful to the late Yasha Rosenfeld for his encouragement of our work. We thank Dezső Boda for providing the Monte Carlo simulations used in the figures and Roland Roth for his many valuable comments on the manuscript. This work was supported by grants from NIH (Grant No. T32NS07044 to D.G.) and DARPA (R.S.E. and W.N.).

APPENDIX A: DESCRIPTION OF THE EXAMPLE SHOWN IN FIGS. 1–3

To illustrate the iterative method, we use an example from our previous paper [16]. We choose to use the same example here for the following two reasons.

(1) It is a general and challenging system since it has three ion species, each with a different size and charge.

(2) In this paper, the purpose of the example and the MC simulations is a step-by-step illustration of the iteration method and its convergence (Figs. 1 and 2). In Fig. 3, we also use it to illustrate the consequences of changing one

component of the ES functional. We show in this paper that the iteration method of Ref. [16] and the new ES functional (8) are equivalent (Appendix B). Therefore, it has already been established that the new ES functional compares well to MC simulations [16,20].

For the example, we consider two half-infinite compartments in the planar (slab) geometry brought into contact at $x=0$. As bulk fluids, left compartment ($x<0$) contains $6M$ Ca^{2+} and $24M$ anions with valence $-1/2$, denoted $A^{1/2-}$ (see below), and the right compartment ($x>0$) contains $0.1M$ CaCl_2 . These two compartments are brought into contact and allowed to equilibrate with the restriction that $A^{1/2-}$ are confined to the left compartment with a hard-wall potential; Ca^{2+} and Cl^- are allowed to equilibrate throughout both compartments.

The system is treated as a grand canonical ensemble. $A^{1/2-}$ are assigned a chemical potential corresponding to that in a $6M$ CaA_4 bulk solution that is at the electrostatic potential $\phi(-\infty)$. Ca^{2+} and Cl^- are assigned the chemical potentials corresponding to a $0.1M$ CaCl_2 bulk solution at the electrostatic potential $\phi(\infty)=0$. The excess chemical potentials are calculated with the MSA and $\phi(-\infty)$ is the Donnan potential between the two bulk solutions. In all DFT calculations, the HS component was computed with the ‘‘antisymmetrized’’ excess free energy density of Ref. [12]. $A^{1/2-}$, Ca^{2+} , and Cl^- were given diameters of 0.280, 0.198, and 0.363 nm, respectively.

In this example we use ions of valence $-1/2$ to make a very general electrostatic system: the three ion species have very different $|z_i|$. The origin of this species is the modeling of carboxyl (COO^-) groups of certain amino acids where both oxygens share the ionizing electron. In a charged, hard-sphere fluid model, we chose to model one COO^- groups as two independent $\text{O}^{1/2-}$ ions [16,19].

APPENDIX B: DERIVATION OF THE FIRST-ORDER DIRECT CORRELATION FUNCTION

By definition,

$$c_i^{(1),\text{ES}}(\mathbf{x}) = c_i^{(1),\text{ES}}[\{\rho_k(\mathbf{y})\}; \mathbf{x}] = -\frac{1}{kT} \frac{\delta F_{\text{ES}}}{\delta \rho_i(\mathbf{x})}. \quad (\text{B1})$$

Functional differentiation of Eq. (8) gives

$$\begin{aligned} -kT c_i^{(1),\text{ES}}(\mathbf{x}) \approx & \sum_j \int \frac{\delta F_{\text{ES}}[\{\bar{\rho}_k(\mathbf{y})\}]}{\delta \bar{\rho}_j(\mathbf{x}')} \frac{\delta \bar{\rho}_j(\mathbf{x}')}{\delta \rho_i(\mathbf{x})} d\mathbf{x}' \\ & + \frac{\delta F_{\text{ES}}^{(1)}}{\delta \rho_i(\mathbf{x})} + \frac{\delta F_{\text{ES}}^{(2)}}{\delta \rho_i(\mathbf{x})}. \end{aligned} \quad (\text{B2})$$

The derivative of $F_{\text{ES}}^{(1)}$ is given by

$$\begin{aligned} -\frac{1}{kT} \frac{\delta F_{\text{ES}}^{(1)}}{\delta \rho_i(\mathbf{x})} = & -\frac{1}{kT} \sum_j \int \frac{\delta F_{\text{ES}}^{(1)}}{\delta \bar{c}_j^{(1),\text{ES}}(\mathbf{x}')} \frac{\delta \bar{c}_j^{(1),\text{ES}}(\mathbf{x}')}{\delta \rho_i(\mathbf{x})} d\mathbf{x}' \\ & + \bar{c}_i^{(1),\text{ES}}(\mathbf{x}) - \sum_j \int \bar{c}_j^{(1),\text{ES}}(\mathbf{x}') \frac{\delta \bar{\rho}_j(\mathbf{x}')}{\delta \rho_i(\mathbf{x})} d\mathbf{x}', \end{aligned} \quad (\text{B3})$$

which may be expanded and rearranged to

$$\begin{aligned} -\frac{1}{kT} \frac{\delta F_{\text{ES}}^{(1)}}{\delta \rho_i(\mathbf{x})} = & \bar{c}_i^{(1),\text{ES}}(\mathbf{x}) - \sum_j \int \bar{c}_j^{(1),\text{ES}}(\mathbf{x}') \frac{\delta \bar{\rho}_j(\mathbf{x}')}{\delta \rho_i(\mathbf{x})} d\mathbf{x}' \\ & + \sum_{j,m} \int \int \frac{\delta \bar{c}_j^{(1),\text{ES}}(\mathbf{x}')}{\delta \bar{\rho}_m(\mathbf{x}'')} \Delta \rho_j(\mathbf{x}') \frac{\delta \bar{\rho}_m(\mathbf{x}'')}{\delta \rho_i(\mathbf{x})} \\ & \times d\mathbf{x}' d\mathbf{x}'', \end{aligned} \quad (\text{B4})$$

where

$$\Delta \rho_k(\mathbf{x}) = \rho_k(\mathbf{x}) - \bar{\rho}_k(\mathbf{x}). \quad (\text{B5})$$

The derivative of $F_{\text{ES}}^{(2)}$ is given by

$$\begin{aligned} \frac{\delta F_{\text{ES}}^{(2)}}{\delta \rho_i(\mathbf{x})} = & \sum_{k,m} \int \int \frac{\delta F_{\text{ES}}^{(2)}}{\delta \bar{c}_{km}^{(2),\text{ES}}(\mathbf{x}', \mathbf{x}'')} \frac{\delta \bar{c}_{km}^{(2),\text{ES}}(\mathbf{x}', \mathbf{x}'')}{\delta \rho_i(\mathbf{x})} d\mathbf{x}' d\mathbf{x}'' \\ & + \sum_k \int \frac{\delta F_{\text{ES}}^{(2)}}{\delta \Delta \rho_k(\mathbf{x}')} \frac{\delta \Delta \rho_k(\mathbf{x}')}{\delta \rho_i(\mathbf{x})} d\mathbf{x}' \\ & + \sum_m \int \frac{\delta F_{\text{ES}}^{(2)}}{\delta \Delta \rho_m(\mathbf{x}'')} \frac{\delta \Delta \rho_m(\mathbf{x}'')}{\delta \rho_i(\mathbf{x})} d\mathbf{x}''. \end{aligned} \quad (\text{B6})$$

Since

$$-2 \frac{\delta F_{\text{ES}}^{(2)}}{kT \delta \bar{c}_{km}^{(2),\text{ES}}(\mathbf{x}', \mathbf{x}'')} = \Delta \rho_k(\mathbf{x}') \Delta \rho_m(\mathbf{x}''), \quad (\text{B7})$$

$$\frac{\delta \bar{c}_{km}^{(2),\text{ES}}(\mathbf{x}', \mathbf{x}'')}{\delta \rho_i(\mathbf{x})} = \sum_j \int \frac{\delta \bar{c}_{km}^{(2),\text{ES}}(\mathbf{x}', \mathbf{x}'')}{\delta \bar{\rho}_j(\mathbf{x}''')} \frac{\delta \bar{\rho}_j(\mathbf{x}''')}{\delta \rho_i(\mathbf{x})} d\mathbf{x}''', \quad (\text{B8})$$

$$-2 \frac{\delta F_{\text{ES}}^{(2)}}{kT \delta \Delta \rho_k(\mathbf{x}')} = \sum_m \int \bar{c}_{km}^{(2),\text{ES}}(\mathbf{x}', \mathbf{x}'') \Delta \rho_m(\mathbf{x}'') d\mathbf{x}'', \quad (\text{B9})$$

$$-2 \frac{\delta F_{\text{ES}}^{(2)}}{kT \delta \Delta \rho_m(\mathbf{x}'')} = \sum_k \int \bar{c}_{km}^{(2),\text{ES}}(\mathbf{x}', \mathbf{x}'') \Delta \rho_k(\mathbf{x}') d\mathbf{x}', \quad (\text{B10})$$

$$\frac{\delta \Delta \rho_k(\mathbf{x}')}{\delta \rho_i(\mathbf{x})} = \delta_{ik} \delta(\mathbf{x} - \mathbf{x}') - \frac{\delta \bar{\rho}_k(\mathbf{x}')}{\delta \rho_i(\mathbf{x})}, \quad (\text{B11})$$

and

$$\begin{aligned} \bar{c}_{ij}^{(2),\text{ES}}(\mathbf{x}, \mathbf{x}') = & \frac{\delta^2 F_{\text{ES}}[\{\bar{\rho}_k(\mathbf{y})\}]}{\delta \bar{\rho}_i(\mathbf{x}) \delta \bar{\rho}_j(\mathbf{x}')} = \frac{\delta^2 F_{\text{ES}}[\{\bar{\rho}_k(\mathbf{y})\}]}{\delta \bar{\rho}_j(\mathbf{x}') \delta \bar{\rho}_i(\mathbf{x})} \\ = & \bar{c}_{ji}^{(2),\text{ES}}(\mathbf{x}', \mathbf{x}), \end{aligned} \quad (\text{B12})$$

we have

$$\begin{aligned}
-\frac{1}{kT} \frac{\delta F_{\text{ES}}^{(2)}}{\delta \rho_i(\mathbf{x})} &= \sum_k \int \bar{c}_{ik}^{(2),\text{ES}}(\mathbf{x}, \mathbf{x}') \Delta \rho_k(\mathbf{x}') d\mathbf{x}' - \sum_{k,m} \int \int \bar{c}_{km}^{(2),\text{ES}}(\mathbf{x}', \mathbf{x}'') \Delta \rho_m(\mathbf{x}'') \frac{\delta \bar{\rho}_k(\mathbf{x}')}{\delta \rho_i(\mathbf{x})} d\mathbf{x}' d\mathbf{x}'' \\
&+ \frac{1}{2} \sum_{j,k,m} \int \int \int \frac{\delta \bar{c}_{km}^{(2),\text{ES}}(\mathbf{x}', \mathbf{x}'')}{\delta \bar{\rho}_j(\mathbf{x}''')} \frac{\delta \bar{\rho}_j(\mathbf{x}''')}{\delta \rho_i(\mathbf{x})} \Delta \rho_k(\mathbf{x}') \Delta \rho_m(\mathbf{x}'') d\mathbf{x}' d\mathbf{x}'' d\mathbf{x}'''. \quad (\text{B13})
\end{aligned}$$

We now have two formulations of the first-order ES DCF: the one used in Ref. [16] given by Eq. (6) and the one given by Eqs. (B2), (B4), and (B13). Comparing these relations shows that there are several extra terms in the latter formulation. We now show that the additional terms cancel exactly for a general functional dependence of $\bar{\rho}_k(\mathbf{x}')$ on $\{\rho_i(\mathbf{x})\}$. Therefore, explicitly accounting for the RFD functional (7) is equivalent to the iteration method.

We start with definitions (12), (13), and

$$\frac{\delta \bar{c}_{km}^{(2),\text{ES}}(\mathbf{x}', \mathbf{x}'')}{\delta \bar{\rho}_j(\mathbf{x}''')} = \bar{c}_{kmj}^{(3),\text{ES}}(\mathbf{x}', \mathbf{x}'', \mathbf{x}''') \quad (\text{B14})$$

to rewrite the first-order DCF (B2):

$$c_i^{(1),\text{ES}}(\mathbf{x}) \approx \sum_j \int \bar{c}_i^{(1),\text{ES}}(\mathbf{x}') \frac{\delta \bar{\rho}_j(\mathbf{x}')}{\delta \rho_i(\mathbf{x})} d\mathbf{x}' - \frac{1}{kT} \frac{\delta F_{\text{ES}}^{(1)}}{\delta \rho_i(\mathbf{x})} - \frac{1}{kT} \frac{\delta F_{\text{ES}}^{(2)}}{\delta \rho_i(\mathbf{x})}, \quad (\text{B15})$$

where

$$-\frac{1}{kT} \frac{\delta F_{\text{ES}}^{(1)}}{\delta \rho_i(\mathbf{x})} = \bar{c}_i^{(1),\text{ES}}(\mathbf{x}) - \sum_j \int \bar{c}_i^{(1),\text{ES}}(\mathbf{x}') \frac{\delta \bar{\rho}_j(\mathbf{x}')}{\delta \rho_i(\mathbf{x})} d\mathbf{x}' + \sum_{j,m} \int \int \bar{c}_{jm}^{(2),\text{ES}}(\mathbf{x}', \mathbf{x}'') \Delta \rho_j(\mathbf{x}') \frac{\delta \bar{\rho}_m(\mathbf{x}'')}{\delta \rho_i(\mathbf{x})} d\mathbf{x}' d\mathbf{x}'' \quad (\text{B16})$$

and

$$\begin{aligned}
-\frac{1}{kT} \frac{\delta F_{\text{ES}}^{(2)}}{\delta \rho_i(\mathbf{x})} &= \sum_k \int \bar{c}_{ik}^{(2),\text{ES}}(\mathbf{x}, \mathbf{x}') \Delta \rho_k(\mathbf{x}') d\mathbf{x}' - \sum_{k,m} \int \int \bar{c}_{km}^{(2),\text{ES}}(\mathbf{x}', \mathbf{x}'') \Delta \rho_m(\mathbf{x}'') \frac{\delta \bar{\rho}_k(\mathbf{x}')}{\delta \rho_i(\mathbf{x})} d\mathbf{x}' d\mathbf{x}'' \\
&+ \frac{1}{2} \sum_{j,k,m} \int \int \int \bar{c}_{kmj}^{(3),\text{ES}}(\mathbf{x}', \mathbf{x}'', \mathbf{x}''') \frac{\delta \bar{\rho}_j(\mathbf{x}''')}{\delta \rho_i(\mathbf{x})} \Delta \rho_k(\mathbf{x}') \Delta \rho_m(\mathbf{x}'') d\mathbf{x}' d\mathbf{x}'' d\mathbf{x}'''. \quad (\text{B17})
\end{aligned}$$

Adding these together and using relation (B12) gives

$$\begin{aligned}
c_i^{(1),\text{ES}}(\mathbf{x}) &\approx \bar{c}_i^{(1),\text{ES}}(\mathbf{x}) + \sum_j \int \bar{c}_{ij}^{(2),\text{ES}}(\mathbf{x}, \mathbf{x}') \Delta \rho_j(\mathbf{x}') d\mathbf{x}' \\
&+ \frac{1}{2} \sum_{j,k,m} \int \int \int \bar{c}_{kmj}^{(3),\text{ES}}(\mathbf{x}', \mathbf{x}'', \mathbf{x}''') \frac{\delta \bar{\rho}_j(\mathbf{x}''')}{\delta \rho_i(\mathbf{x})} \Delta \rho_k(\mathbf{x}') \Delta \rho_m(\mathbf{x}'') d\mathbf{x}' d\mathbf{x}'' d\mathbf{x}'''. \quad (\text{B18})
\end{aligned}$$

Although we do not show it, by continuing this process for successive terms in the *untruncated* series (4), the last term in Eq. (B18) is canceled by the next term in the series because of the relation

$$\bar{c}_{kmj}^{(3),\text{ES}}(\mathbf{x}', \mathbf{x}'', \mathbf{x}''') = \bar{c}_{mkj}^{(3),\text{ES}}(\mathbf{x}'', \mathbf{x}', \mathbf{x}''') = \bar{c}_{jmk}^{(3),\text{ES}}(\mathbf{x}''', \mathbf{x}'', \mathbf{x}'). \quad (\text{B19})$$

Thus we conclude that all the terms that include functional derivatives of $\bar{\rho}_j(\mathbf{x}')$ cancel and that

$$c_i^{(1),\text{ES}}(\mathbf{x}) \approx \bar{c}_i^{(1),\text{ES}}(\mathbf{x}) + \sum_j \int \bar{c}_{ij}^{(2),\text{ES}}(\mathbf{x}, \mathbf{x}') \Delta \rho_j(\mathbf{x}') d\mathbf{x}' \quad (\text{B20})$$

with the DCFs $\bar{c}_i^{(1),\text{ES}}(\mathbf{x})$ and $\bar{c}_{ij}^{(2),\text{ES}}(\mathbf{x}, \mathbf{x}')$ given by Eqs. (12) and (13). This result is *not* true for any general ES functional $G[\rho_j(\mathbf{x}), \bar{\rho}_j(\mathbf{x}')]];$ if $\bar{\rho}_j(\mathbf{x}')$ is a itself a functional of $\rho_j(\mathbf{x})$, then the extra terms created in the first-order DCF by the new functional dependence (16) cancel because we start with a Taylor series expansion of the free energy in Eq. (4).

- [1] E. Waisman and J.L. Lebowitz, *J. Chem. Phys.* **52**, 4307 (1970); **56**, 3086 (1972); **56**, 3093 (1972); L. Blum, *Mol. Phys.* **30**, 1529 (1975).
- [2] J.M.J. van Leeuwen, J. Groeneveld, and J. deBoer, *Physica* **25**, 792 (1959); E. Meeron, *J. Math. Phys.* **1**, 192 (1960); T. Morita, *Prog. Theor. Phys.* **23**, 829 (1960); G.S. Rushbrooke, *Physica* **26**, 259 (1960); L. Verlet, *Nuovo Cimento* **18**, 77 (1960).
- [3] R. Roth and S. Dietrich, *Phys. Rev. E* **62**, 6926 (2000).
- [4] D. Goulding, S. Melchionna, and J.-P. Hansen, *Phys. Chem. Chem. Phys.* **3**, 1644 (2001).
- [5] L. Mier-y-Teran, S.H. Suh, H.S. White, and H.T. Davis, *J. Chem. Phys.* **92**, 5087 (1990).
- [6] Z. Tang, L.E. Scriven, and H.T. Davis, *J. Chem. Phys.* **97**, 494 (1992); **97**, 9258 (1992); **100**, 4527 (1994).
- [7] T. Biben, J.-P. Hansen, and Y. Rosenfeld, *Phys. Rev. E* **57**, R3727 (1998).
- [8] D. Boda, D. Henderson, R. Rowley, and S. Sokołowski, *J. Chem. Phys.* **111**, 9382 (1999); D. Boda, D. Henderson, A. Patrykiewicz, and S. Sokołowski, *ibid.* **113**, 802 (2000).
- [9] R. Evans, in *Fundamentals of Inhomogeneous Fluids*, edited by D. Henderson (Marcel Dekker, New York, 1992).
- [10] Y. Rosenfeld, *Phys. Rev. Lett.* **63**, 980 (1989).
- [11] Y. Rosenfeld, *J. Chem. Phys.* **98**, 8126 (1993).
- [12] Y. Rosenfeld, M. Schmidt, H. Löwen, and P. Tarazona, *Phys. Rev. E* **55**, 4245 (1997).
- [13] R. Roth, R. Evans, A. Lang, and G. Kahl, *J. Phys.: Condens. Matter* **14**, 12063 (2002).
- [14] R. Penfold and S. Nordholm, *J. Chem. Phys.* **96**, 3102 (1992); R. Penfold, B. Jönsson, and S. Nordholm, *ibid.* **99**, 497 (1993).
- [15] L.J.D. Frink, A. Thompson, and A.G. Salinger, *J. Chem. Phys.* **112**, 7564 (2000).
- [16] D. Gillespie, W. Nonner, and R.S. Eisenberg, *J. Phys.: Condens. Matter* **14**, 12129 (2002).
- [17] B. Eisenberg, *Biophys. Chem.* **100**, 507 (2003).
- [18] B. Hille, *Ion Channels of Excitable Membranes*, 3rd ed. (Sinauer, Sunderland, MA, 2001).
- [19] W. Nonner and B. Eisenberg, *Biophys. J.* **75**, 1287 (1998); W. Nonner, L. Catacuzzeno, and B. Eisenberg, *ibid.* **79**, 1976 (2000); W. Nonner, D. Gillespie, D. Henderson, and B. Eisenberg, *J. Phys. Chem. B* **105**, 6427 (2001).
- [20] Unpublished comparisons to the Monte Carlo simulation results of Boda *et al.* [8].
- [21] K. Hiroike, *Mol. Phys.* **33**, 1195 (1977).
- [22] L. Blum and Y. Rosenfeld, *J. Stat. Phys.* **63**, 1177 (1991).
- [23] W.H. Press, S.A. Teukolsky, W.T. Vetterling, and B.P. Flannery, *Numerical Recipes in C: The Art of Scientific Computing*, 2nd ed. (Cambridge University Press, Cambridge, UK, 1992).
- [24] L. Blum, in *Theoretical Chemistry: Advances and Perspectives*, edited by H. Eyring and D. Henderson (Academic Press, New York, 1980), Vol. 5.
- [25] R. Roth (private communication).